Detecting Neuropathy Using Measures of Motor Unit Activation Extracted from Standard Concentric Needle Electromyographic Signals

Meena AbdelMaseeh[1], Benn Smith[2], and Daniel Stashuk[1]

Abstract*— *Objective: **Motor unit loss associated with neuropathic disorders affects motor unit activation. Quantitative electromyographic (EMG) features of motor unit activation estimated from the sequences of motor unit potentials (MUPs) created by concurrently active motor units can support the detection of neuropathic disorders. Interpretation of most motor unit activation feature values are, however, confounded by uncertainty regarding the level of muscle activation during EMG signal detection. A set of new features circumventing these limitations are proposed, and their utility in detecting neuropathy is investigated using simulated and clinical EMG signals.**

Methods: **The firing sequence of a motor neuron was simulated using a compartmentalized Hodgkin-Huxley based model. A pool of motor neurons was modelled such that each motor neuron was subjected to a common level of activation. The detection of the firing sequence of a motor neuron using a clinically detected EMG signal was simulated using a model of muscle anatomy combined with a model representing muscle fiber electrophysiology and the voltage detection properties of a concentric needle electrode.**

Significance: **Findings are based on simulated EMG data representing 30 normal and 30 neuropathic muscles as well as clinical EMG data collected from the tibialis anterior muscle of 48 control subjects and 30 subjects with neuropathic disorders. These results demonstrate the possibility of detecting neuropathy using motor unit recruitment and mean firing rate feature values estimated from standard concentric needle detected EMG signals.**

I. Introduction

Needle electromyography and nerve conduction studies are physiological gold standards for detecting neuromuscular disorders and determining whether these disorders are likely to be due to myopathic, neuropathic or neuromuscular junction (NMJ) related processes. The clinical practice of analyzing electromyographic (EMG) signals can be classified broadly into qualitative, semi-quantitative or quantitative.

Quantitative analysis starts by clustering detected motor unit potentials (MUPs) acquired during slight voluntary isometric muscle contraction into distinct motor unit potential trains (MUPTs), based on the assumption that MUPs from a single motor unit are expected to show less morphological variation than MUPs from other MUs [12]. Each MUPT is represented by an estimated MUP template and the ensemble of MUPs comprising the MUPT. A set of quantitative electromyograhic (QEMG) features are then extracted to characterize average MUP morphology, the consistency of the morphologies of the individual MUPs belonging to the MUPT and motor unit (MU) recruitment and firing pattern [2]. MUPT characterizations can be used to determine whether a disorder of nerve or muscle is likely and, if so, whether it is mild or severe [1].

The amount of force produced by a muscle is controlled by activating or deactivating MUs and by modulating the firing rates of active MUs. Neuropathic processes can change the number, territory, and contractile properties of MUs. These pathological changes are in turn expected to induce changes in MU activation patterns [5]. Therefore, QEMG features estimated from the sequences of firing times of MUPs created by concurrently active MUs are likely to be useful for detecting neuropathy.

Earlier studies have evaluated the discriminability of MU mean interdischarge intervals (IDIs) and their standard deviation using MUPTs extracted from EMG signals detected using a single fiber needle electrode [4], [6]. A single fiber needle electrode was used, because the selectivity of this electrode allows the signals detected to be more reliably decomposed into their constituent MUPTs.

Results from both of these studies demonstrated that neuropathic muscles had decreased mean IDI and higher IDI variability. Similar results were obtained in [3] using a standard concentric needle electrode. In all these studies, the level of contraction was measured and controlled.

Unlike these studies and others reported in the literature, this work attempts to answer questions that, from a clinical perspective, are more practical: (1) Can we extract discriminating QEMG MU recruitment and firing rate features from EMG signals detected using a conventional clinical concentric needle electrode? (2) Can this be achieved using a clinically practical signal acquisition protocol that is also suitable for extraction of morphological features? (3) Can these QEMG features be extracted automatically, quickly, accurately and using a procedure the output of which can be evaluated and validated by a physician?

These questions have been addressed through the analysis of simulated and clinical EMG studies. Analyzing simulated data is useful because it overcomes many inherent limitations of clinical data such as labeling inaccuracies, non-uniformity of disease involvement, acquisition dependence (such as needle focusing and instrumentation noise) and incompleteness of extracted MUPTs. Simulation can also provide clearer insight by excluding irrelevant phenomena and factors, such as MUP instability caused by NMJ jitter, and by modeling other relevant parameters that are very difficult to measure

[1]D. Stashuk and M. AbdelMaseeh are with the department of Systems Design Engineering, University of Waterloo, Waterloo, ON, Canada stashuk at uwaterloo.ca

[2]B. Smith is with the Department of Neurology, Mayo Clinic, Scottsdale, AZ, USA

978-1-4244-7929-0/14/$26.00 ©2014 IEEE

Component	Description
Motor Neuron: $s_j(t) = f_{\text{neuron}}(a_j, \overline{g}_{ex})$	$s_j(t)$ is the firing sequence of the j^{th} MN. $s_j(t)$ is a function of the soma-dendritic equivalent cylinder diameter a_j of the MN and the steady excitatory inputs to the different dendritic compartments $\overline{g}_{ex}$ of the MN.
Fiber Potential: $p_i(t) = f_{\text{MFP}}(d_i, \overline{c}_i, n_i, \overline{e})$	$p_i(t)$ is the MFP of the i^{th} muscle fiber as detected by a concentric needle electrode placed at $\overline{e}$. $p_i(t)$ is a function of muscle fiber diameter d_i, center location $\overline{c}_i$, and neuro-muscular junction (NMJ) location n_i.

TABLE I

FUNCTIONAL DESCRIPTION OF THE DYNAMIC COMPONENT MODELS. NOTE THAT INSIGNIFICANT PARAMETERS AND THOSE ASSUMED TO BE FIXED ARE EXCLUDED FROM THE LISTS OF INPUT PARAMETERS. SCALARS ARE NOTATED AS LOWER CASE VARIABLES, VECTORS AS LOWER CASE VARIABLES WITH AN OVERLINE, WHILE MATRICES ARE NOTATED AS UPPERCASE VARIABLES WITH AN OVERLINE

Component	Description
Muscle Layout: $[\overline{d}, \overline{c}, \overline{n}, \overline{W}] = f_{\text{layout}}(N_{\text{MU}}, \overline{e})$	Muscle layout is defined by the MF diameters $\overline{d}$, center locations $\overline{c}$, NMJ locations $\overline{n}$ and the MF assignments to the N_{MU} MUs. The specific MF to MU assignments are represented using matrix $\overline{W}$. The needle location $\overline{e}$ is an input parameter because needle insertion causes nearby fibers to be pushed aside.
Neuropathy: $\overline{W'} = f_{\text{neuro}}(\overline{d}, \overline{c}, \overline{W}, \gamma, \delta)$	Neuropathy causes a loss of a γ fraction of the MNs and MF reinnervation, i.e. reassignment of the MFs from the lost MNs to surviving MNs, represented by matrix ($\overline{W'}$), such that a surviving MN can innervate up to δ percent more muscle fibers.
Motor Neuron Pool: $\overline{a} = f_{\text{pool}}(\overline{t})$	The MU territory radii of the corresponding MUs $\overline{a}$ belonging to the pool are modeled as a function of the muscle force $\overline{t}$ at which the MNs are recruited.

TABLE II

FUNCTIONAL DESCRIPTION OF THE STRUCTURAL COMPONENT MODELS.

experimentally, namely excitatory input to a motor neuron (MN) pool.

Several models related to different aspects of low level isometric skeletal muscle contraction have been developed with different inputs, outputs, and level of detail to serve different objectives. For instance, a detailed model of a MN pool was built to answer neurophysiological questions such as the schema of input distribution in [14], [15]. Nandedkar [9], [10] devised a model focusing on electrode properties and muscle fiber potentials (MFPs) to contrast the spatial selectivity of different electrodes and the relationship between muscle fiber (MF) anatomy and detected EMG signal features.

Models in [7] proposed a detailed muscle layout to investigate EMG signal decomposition and analysis in a structured manner. In this work, these models of Traub, Nandedkar and Hamilton-Wright are combined to simulate the detection of MN firings using concentric needle-detected EMG signals.

II. COMPOSITE MODEL CONSTRUCTION

A. Modularized Architecture

To simulate the use of concentric-needle-detected EMG signals to quantify MN activity, the parts of the human neuromuscular system that control MN activation and the parts of the acquisition and analysis systems that influence the estimation of the corresponding MU activation features were independently modelled and subsequently combined into a composite model composed of modularized functional component models. The functional descriptions of the five component models are summarized in Tables I and II.

B. Motor Neuron Model

To provide a basis for the accurate study of the quantification of the firing sequence of a MN, a rigorous and detailed MN model based on previous work completed by [15] was developed. The key advantage of this relatively detailed model is its ability to model MNs having different sizes and input resistances. This model can therefore be used as a building block in a MU pool model.

The main aspects of the developed model are:

- MN morphology and membrane heterogeneity are represented by 5 compartments comprised of 3 dendritic compartments (proximal, middle, and distal), the soma, and the initial segment. The dendritic tree is converted into an equivalent cylinder using the method of Rall [11].
- The membrane of a dendrite is passive, while the time and voltage dependence of potassium and sodium conductance of the active membrane compartments (the soma and the initial segment) are modeled using Hodgkin-Huxley like equations modified to match voltage clamp data.
- The after hyper-polarization following an action potential in a MN is realized using a slow potassium conductance.
- The inputs to the model are restricted to excitatory synaptic conductance values $\overline{g}_{ex}$ associated with the 3 dendritic compartments.

The radii of the soma equivalent cylinder and the dendritic equivalent cylinder are set equal. It was shown that this radius a can be estimated from a set of preset values (membrane resitivity R_m, internal resistivity R_i, equivalent length of the soma-dendritic length L, and characteristic length λ) and the input resistance R_{input} using the following formula:

$$a = \left[\frac{R_m R_i}{2}\right]^{1/3} \times \left[\frac{coth(L/\lambda)}{\pi R_{\text{input}}}\right]^{2/3} \quad (1)$$

The resulting system of 15 coupled differential equations is solved using the Runge-Kutta method with a variable time step.

C. Motor Neuron Pool Model

In [14], it was shown that the threshold force of activation (h) in grams, i.e., the force at which a MN is recruited, can

be modelled as a function of the recruitment order j of the MN using:

$$h = 1000 - 469 \times \log(j) \tag{2}$$

R_{input} in MΩ is then estimated using:

$$R_{\text{input}} = 2.5 - \frac{h}{600} \tag{3}$$

and the potassium slow conductance time constant in ms as:

$$\frac{1}{\beta_q} = 13.3 + 6.7 \times R_{\text{input}} \tag{4}$$

D. Muscle Model

The activity of a MN can be determined by detecting MUPs produced by its muscle fibers. Therefore, if the MUPs associated with the activity of a MN can be consistently detected in an acquired needle-detected EMG signal, the extracted MUPT is defined as decomposable and can be used to estimate statistics related to the firing sequence of the MN. The simulation of a MFP $p_i(t)$ as detected by a needle electrode requires determining the diameter of the muscle fiber and the location of the muscle fiber and its NMJ relative to the electrode detection surface. Therefore, the muscle layout model of [7] which specifies the diameter d, center $\overline{c}$ and NMJ n location of each fiber as well as its associated MU $\overline{W}$ was used. The main stages of simulating a muscle layout can be summarized as:

1-Assigning MU territory diameter: Both the muscle and the constituent MU territories are assumed to have circular cross-sectional areas. The MU sizes are sampled from a Poisson distribution.

2-Assigning MU territory center: The two main assumptions are: (1) there is no correlation between MU territory diameter and MU territory center, and (2) MU centers are uniformly distributed across the cross-sectional area of a muscle. The algorithm developed in [7] which divides the muscle cross section into a uniform grid was used. This algorithm then iteratively places MU territory centres at grid points, perturbed by random offsets, in a randomized manner guaranteeing that any MU is equally likely to be placed in any quadrant.

3-Assigning MF center location $\overline{c}$: MFs are located in a uniform grid such that a uniform density of 400 MF/mm^2 is achieved.

4-Assigning MFs to MUs ($\overline{W}$): Each MF is assigned randomly to one of the MUs which has territory including its location. The likelihood of the i^{th} MF being assigned to the j^{th} MU is estimated as a weighted sum of three factors: (1) the distance from the MU territory center to the MF center, (2) the number of fibers already assigned to the MU (3) the expected number of MFs to be assigned to the MU.

5-Assigning MF diameter d: The diameters of the MFs belonging to a given MU are sampled from a Gaussian distribution specific to the MU. The mean MF diameter of a MU is modified by a range of increments to account for the fact that type-I fibers are more likely to be found in smaller MUs.

6-Assigning NMJ location n: Because a muscle cross-section is arbitrarily chosen to be in a x-y plane, the location of the NMJ is modelled to be along the z axis and is drawn from a Gaussian distribution with a 0 mean and a standard deviation based on its MU territory diameter.

6-MF ploughing: A concentric needle electrode detection surface is modeled as an ellipsoidal cross-sectional area at the tip of the needle oriented at 15.95 degrees relative to the axis of the cannula. When simulating detected EMG signals the needle tip is assumed to be positioned at a specific location $\overline{e}$ within the muscle and all MFs that would intersect with the cannula are therefore assumed to have moved either above or below the cannula, whichever is closer.

The MN pool model is interfaced to this muscle model by assigning MNs ordered according to their recruitment threshold to MUs ordered based on their territory diameters.

E. Muscle Fiber Potential Model

The model used to simulate MFPs is based on the work done in [9], [10]. The concentric needle electrode is assumed to have an ellipsoid detection surface with a major axis of 580 μm and a minor axis of 150 μm. The ellipse is modeled using 6 line integrals spaced equally across the surface. The MFP of the i^{th} fiber $p_i(t)$ is calculated by convolving a propagating transmembrane current with a weight function related to the relative geometry of the detection surface and the fiber location:

- **Propagating transmembrane current** amplitude and conduction velocity are dependent on MF diameter d_i.
- **Electrode weight function** is the average response to a unit impulse current of the 6 line electrode potential response functions used to model the concentric needle detection surface. It is dependent on the position of the electrode $\overline{e}$, the position of the MF center $\overline{c_i}$, NMJ n_i, and conductance properties of the extracellular tissue.

The transmembrane currents traveling toward and away from the electrode based on $\overline{e}$ and the NMJ location n_i are both modeled. For a given position of the electrode detection surface, a MFP is simulated for each fiber of a motor unit. If any of the simulated MFPs of the MU has a second derivative value of greater than 1 kV/s^2, the corresponding MUPT is considered decomposable (i.e. the corresponding MU is considered to have been sampled and the firing sequence of its MN is analyzed).

F. Neuropathy Model

A diffuse neuropathic process is simulated as a loss of MNs [8]. Different levels of involvement are modeled as the loss of different fractions γ of the total number of MNs. It is assumed that all MUs are equally likely to be affected by the diffuse disease process, therefore lost MNs are randomly selected. The re-innervation process is modeled by re-executing the MF assignment procedure described in section II-D. However, a surviving MN can support only a maximum number of additional fibers which is described as a fraction δ of its original size.

III. Data Analysis

A. Estimation of mean MU firing rates

The error-filtered estimation (EFE) algorithm described in [13] was used to estimate mean MU firing rates. This algorithm has been shown to provide accurate estimates even when the firing sequence of a MUPT is only partially complete or includes erroneous firings.

The EFE algorithm makes use of the fact that the probability distribution function of the IDIs of an incomplete and/or an inaccurate firing sequence has a peak corresponding to the true mean IDI and other peaks at integer multiples of the true mean IDI value.

B. Measures of MU Activation

A set of features describing a given contraction is estimated from the extracted MUPTs and their associated MU mean firing rates:

No. of decomposable MUPTs: The number of active MUs sampled during the contraction

Contraction Mean Firing Rate (cont.MFR): Mean of the MU mean firing rates of the MUs sampled during the contraction

Contraction Sum Mean Firing Rate (cont.SFR): Sum of the MU mean firing rates of the active MUs sampled during the contraction

Contraction Mean Firing Rate Range (cont.Range): Difference between the maximum MU mean firing rate and the minimum MU mean firing rate of the active MUs sampled during the contraction

IV. Data Acquistion

A. Clinical Data Acquisition

Routine clinical needle EMG was performed in tibialis anterior (TA) muscles. Following needle positioning to detect suitably sharp MUPs (with rise times $\leq$ 0.5 msec) during low level muscle contraction, a manual semiquantitative assessment of the detected signal was completed. The level of contraction was then increased until 40 to 60 MUPs per second were detected and 15 sec of needle detected signal was acquired. This was repeated at multiple distinct needle positions. Muscles were annotated by an experienced clinical neurophysiologist (BES) as normal or neuropathic based on manual semiquantitative assessments of EMG signals detected during the low level muscle contractions across all sampled needle positions. For each needle position, MUPTs were extracted from EMG signals detected during the increased levels of muscle contraction using a standard DQEMG algorithm [12]. 180 contractions were sampled from 48 normal subjects and decomposed into 838 MUPTs. 108 contractions were sampled from 30 subjects with neuropathic muscles and decomposed into 536 MUPTs. All data was sanitized of personal identifying information.

B. Simulated Data Acquisition

Using the muscle layout model $f_{\text{layout}}(.)$, 60 simulated muscles were generated with each muscle having 120 MUs. 30 of them were modified by the modeled neuropathic process $f_{\text{neuro}}(.)$. γ was set to 0.3 for the first 10 muscles, 0.4 for the second 10, and 0.5 for the last 10. δ was set to 0.5 for all neuropathic simulated muscles. Using the MFP model $f_{\text{MFP}(.)}$, decomposable MUPTs detectable by a concentric needle EMG electrode were identified.

The MN pool model $f_{\text{pool}}(.)$ and the MN model $f_{\text{neuron}}(.)$ do not include any stochastic components, therefore there was no need to rerun them for each muscle and/or excitation level. The sequence of inputs applied to all MNs in the pool was a ramp sequence of excitatory conductance in mmho: $g_{ex}^{(c)}(k) = 1.5 \times 10^{-5} + k \times 10^{-6}$ where $c \in \{1, 2, 3\}$ is the dendritic compartment index and k is a step in the input. At each step, the $\overline{g}_{ex}$ was maintained constant for all MNs for 2 seconds to simulate an isometric contraction.

The first set of inputs was $k \in \{0, 2, ..100\}$. The average cont.SFR of normal simulated muscles was then calculated at each step. The range of steps for which $0 \leq$ avg. cont.SFR ≤ 100 was found to be $2 \leq k \leq 8$. Another fine tuned set of inputs was then created with $k \in \{2, 2.125, 2.25, ..., 8\}$. It was found that MNs of recruitement order $j \leq 85$ were recruited by $k = 8$.

V. Results & Discussion

Results from the clinical and simulated EMG studies shown in Figure 1 demonstrate an increased cont.MFR for neuropathic muscles compared to normal muscles at a given cont.SFR (or No. of decomposable MUPTs). These results are consistent to results reported in [3], [5] and suggest that subsets of the newly proposed features can be used for detection of neuropathy.

The increase in cont.MFR. is relatively higher for cont.SFR. above 40 Hz. The acquisition protocol in which the contraction level is increased until 40 to 80 MUPs/s are detected has already been shown to be efficient in extracting QEMG features capturing MUP morphology and morphological stability [2]. This suggests that these features can be automatically extracted without the need to complete an additional/different acquisition protocol and/or to measure force.

The evidence of neuropathy provided by the newly proposed MU activation features is independent from that provided by morphological features. Therefore, a set of features combining both aspects, i.e., morphological and activation features, is expected to yield more accurate categorizations than a set including either of them individually. Moreover, electrodiagnostic clinicians are familiar with MU mean firing rate concepts and the EFE algorithm estimates can be easily validated by examining the IDI distributions.

It is worth noting that in practice increasing the cont.SFR of an EMG signal above 100 Hz makes decomposition of the EMG signal into its constituent MUPs more difficult because more MUP superpositions are likely to occur.

Based on our simulation results, when cont.SFR is above 20 Hz around 25% of active MUs are decomposable. This might

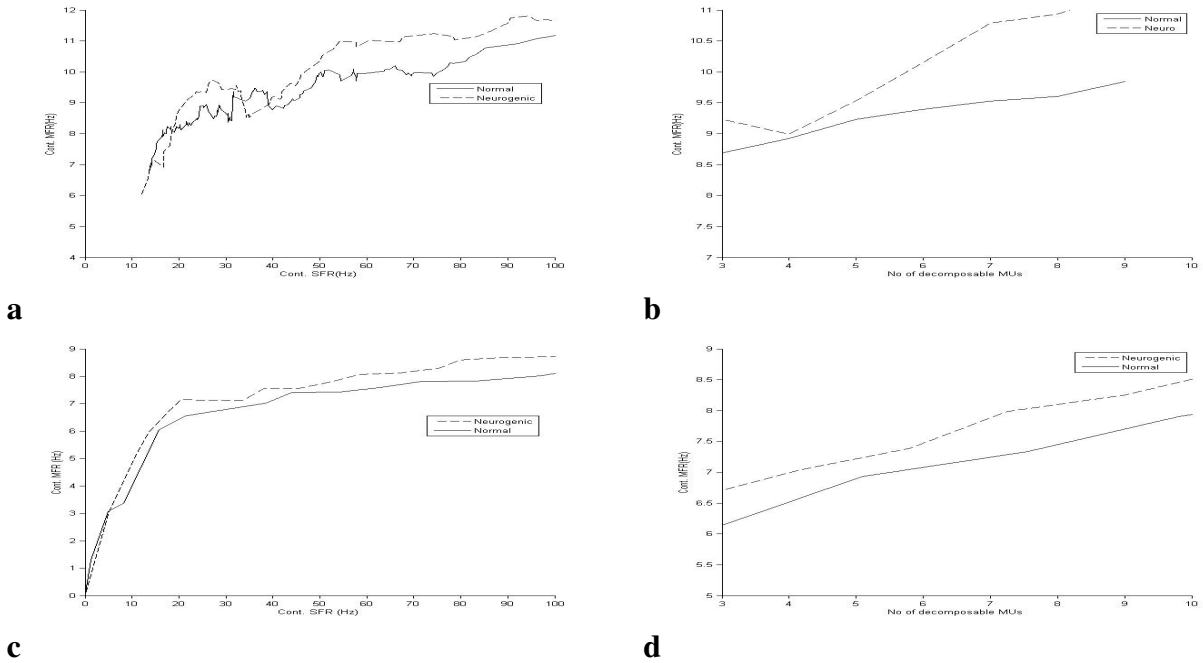

Figure 1: (a) and (b) show the variation of Cont. MFR as the Cont. SFR and No. of decomposable MUs change respectively for clinical EMG studies. (c) and (d) show the results as obtained from simulated studies.

explain why the results obtained using cont.Range did not show clear discriminablity between normal and neuropathic muscles. It is unlikely in normal muscles that MNs reflecting the width of the full range will be sampled.

Three main limitations of the implemented composite model can be summarized as: (1) The MN and MN pool models used excluded some temporal details, such as sensory feedback loops and synaptic neurodyanimcs, that could be useful for muscle characterization. (2) Needle movement and instrumentation noise caused by a subjects inability to maintain a constant contraction were not modelled. (3) The MUP model, as implemented, was not used to analyse MUP morphological features. It is important to investigate potential relationships between aspects of MUP morphology and MU activation.

The firing sequences of concurrently active MUs are too complex to be adequately described using only their mean firing rates. Other measures quantifying the variability of firing rates, synchrony among MUs firings and correlations of their instantaneous firings rates might also yield discriminative information taking into consideration acquisition and analysis limitations. While MUPT features characterize MUs, the features proposed in this study quantify a subset of concurrently active MUs in a given muscle and therefore can be used to characterize the muscle. New methods are being sought to optimize integration of information coming from features describing individual MUs as well as whole muscles.

REFERENCES

[1] Meena AbdelMaseeh, T Chen, Pascal Poupart, Benn Smith, and Daniel Stashuk. Transparent muscle characterization using quantitative electromyography: Different binarization mappings. *Neural Systems and Rehabilitation Engineering, IEEE Transactions on*, 22(3):511–521, 2014.

[2] Meena Abdelmaseeh, Benn Smith, and Daniel Stashuk. Feature selection for motor unit potential train characterization. *Muscle & Nerve*, 49(5):680–690, 2014.

[3] L. Dorfman, J. Howard, and K. McGill. Motor unit firing rates and firing rate variability in the detection of neuromuscular disorders. *Electroencephalography and Clinical Neurophysiology*, 73(3):215 – 224, 1989.

[4] A. Fuglsang-Frederiksen, T. Smith, and H. Hogenhaven. Motor unit firing intervals and other parameters of electrical activity in normal and pathological muscle. *Journal of the Neurological Sciences*, 78(1):51 – 62, 1987.

[5] L. Grimby, K. Holm, and L. Sjustrm. Abnormal use of remaining motor units during locomotion in peroneal palsy. *Muscle & Nerve*, 7(4):327–331, 1984.

[6] J. Halonen, B. Falck, and H. Kalimo. The firing rate of motor units in neuromuscular disorders. *Journal of Neurology*, 225(4):269–276, 1981.

[7] A. Hamilton-Wright and D. Stashuk. Physiologically based simulation of clinical emg signals. *Biomedical Engineering, IEEE Transactions on*, 52(2):171–183, Feb. 2005.

[8] A. Hamilton-Wright, D. Stashuk, and Timothy J. Doherty. Simulation of disease effects on muscle structure, activation and acquired electromyography. *Muscle & Nerve*, 28(S12), 2003.

[9] S. Nandedkar and E. Stålberg. Simulation of single muscle fibre action potentials. *Medical and Biological Engineering and Computing*, 21(2):158–165, 1983.

[10] Sanjeev D. Nandedkar, Donald B. Sanders, Erik V. Stålberg, and Steen Andreassen. Simulation of concentric needle emg motor unit action potentials. *Muscle & Nerve*, 11(2):151–159, 1988.

[11] W. Rall. Theory of physiological properties of dendrites. *Annals of the New York Academy of Sciences*, 96(4), 1962.

[12] D. Stashuk. Emg signal decomposition: how can it be accomplished and used? *Journal of Electromyography and Kinesiology*, 11(3):151 – 173, 2001.

[13] D. Stashuk and Y. Qu. Robust method for estimating motor unit firing-pattern statistics. *Medical and Biological Engineering and Computing*, 34(1):50–57, 1996.

[14] R. Traub. A model of a human neuromuscular system for small isometric tensions. *Biological Cybernetics*, 26(3):159–167, 1977.

[15] R. Traub. Motorneurons of different geometry and the size principle. *Biol Cybern*, 25(3):163–176, Feb 1977.